

Investigation of Thermal and Solar Properties of Aerogel Powder Coated Textiles

Atike KOKEN^{1,2*}, Mehmet KANİK¹

¹ Department of Textile Engineering, Bursa Uludag University, 16059, Bursa, Turkey

² Technology Transfer Office, Bursa Technical University, 16310, Bursa, Turkey

<http://doi.org/10.5755/j02.ms.32869>

Received 5 December 2022; accepted 1 January 2023

Aerogels, the lowest-density solids in the world, have very effective thermal insulation properties with their extremely high surface area and porous structure. Recently, there has been an increasing interest in using aerogels in the textile industry, especially to obtain functional and technical textiles. In this study, thermal and solar properties of polyester fabrics coated at different concentrations (1 %, 2 %, and 4 %) of aerogels with different particle sizes ($\sim 8 \mu\text{m}$, 0–80 μm , 0–0.5 mm) were investigated. It was observed that the aerogel particle size and concentration had a significant effect on the thermal and solar properties, and the lowest thermal conductivity coefficient and thermal resistance values (0.036 W/mK and 14.33 m² K/W, respectively) appeared at the largest particle size and maximum concentration. In contrast, the solar reflectance values of the coated samples decrease up to 62 % with increasing aerogel particle size. In a conclusion, the coating method with aerogel powders could be applied to improve the thermal insulation and solar protection properties of mainly curtains, tents, tarpaulins, and sportswear fabrics.

Keywords: aerogels, thermal insulation, solar protection, technical textiles, coatings.

1. INTRODUCTION

Recently, textile materials have been in a state of significant transformation through research and technological developments. They are being produced as technical materials and attract people's attention with their important functional properties like high tenacity, flame retardancy, waterproofing, heat insulation, antibacterial, antifungal, etc. Advances in material technologies are an important driving force for producing functional textiles. These functional properties are achieved with different processes (coating, spraying, sol-gel, plasma treatment, ultraviolet (UV) curing, and microencapsulation, etc.) [1, 2] and different new materials (graphene, carbon nanotubes, nanomaterials, and biomaterials, etc.) [3, 4]. One of the new material groups is aerogels which are an impressive and ultralight material group. Kistler discovered aerogels in 1931 [5] and in the literature, there have been many studies on the development of aerogels since then. Most studies belong to the period after 1990 when the research accelerated. Aerogels have the lowest thermal conductivity and density in the world [6, 7].

Aerogels are synthesized by the sol-gel technique that consists of three steps: a) gel formation, b) aging, and c) solvent removal (drying) [8]. Aerogel surface area and pore size can be changed with the parameters at these gel stages. Aerogels produced by the selection of different parameters such as the type of materials and catalysts used as initiating materials in the synthesis of aerogels, pH values and drying temperature show very different properties [9, 10]. They are advanced materials with a melting temperature above 1200 °C. The heat conduction mechanisms of aerogels are based on three ways: a) heat transfer over the solid skeleton, b) heat transfer over the gas phase, and c) radiation heat

transfer over particles. The gas or air movement is limited in the aerogels and due to their high porosity and nano-sized pores, aerogels have low thermal conductivity coefficients up to half the air's average [11, 12]. The thermal conductivity coefficients of some selected thermal insulation materials and silica aerogels are given in Table 1 [7, 12, 13].

Table 1. Thermal conductivity coefficients of materials [7, 12, 13]

Material	Thermal conductivity coefficient, W/mK
Air	0.026
Silica aerogel	0.018
Rock wool	0.040
Glass wool	0.038
Extruded polystyrene (XPS)	0.030
Polyurethane foam	0.024
Cellular glass	0.024
Perlite (expanded)	0.045

Silica aerogels are the most widely produced and used groups in aerogels because of raw materials which can easily be found in nature. As well as silica aerogels have a low solid silica content, resulting in a low thermal conductivity coefficient and therefore less heat conduction. Due to these properties, aerogels are used in many different sectors and applications such as insulation, construction, chemistry, electronics, energy, biomedical, agriculture, filtration, and textiles etc. (Fig. 1) [14, 15].

Studies on the application of aerogels to textile materials generally started to increase after 2000 [16, 17]. Aerogels are applied to textile materials to achieve more functionality, especially thermal insulation. There are different application methods to provide functional textile materials with aerogels. These methods vary according to

* Corresponding author. Tel.: +90-224-808 10 97.
E-mail: atike.koken@btu.edu.tr (A. Koken)

the structures of textile materials, additives, auxiliary chemicals and application areas.

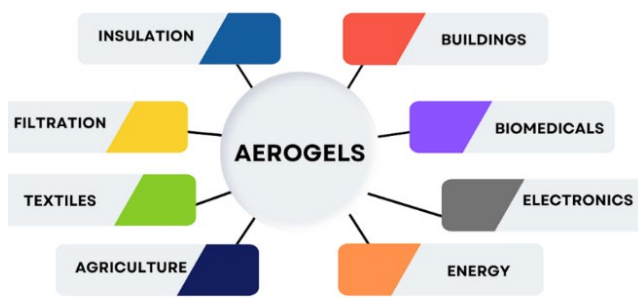


Fig. 1. Application areas of aerogels

One of the most common application methods is incorporating aerogels into nonwoven surfaces. As a result of this method, commercial insulation products are produced in felt forms which are widely used especially in building thermal insulation, production machines operating under high temperatures and heat transmission lines, and firefighter suits [18–22]. Apart from these, as a striking example, the study of aerogels to obtain special space suits for low temperatures is mentioned by the NASA Spinoff Company [23]. As a different field, it has been used in boots that keep the feet warm even at low temperatures at high altitudes in mountaineering sports [24]. Research on providing thermal insulation by a coating of aerogels on textile fabrics is quite limited [22, 25–27], and there is no specific study in the literature on the simultaneous evaluation of aerogel particle sizes and concentrations in the aerogel-coated fabrics. This research aim is to investigate the effect of particle size and concentration of silica aerogel powders on the thermal and solar properties of coated textiles. The coated textiles obtained by this study would be able to use in different application areas such as tents, curtains, cold weather jackets, and insulation materials for high-heat pieces of machinery.

2. EXPERIMENTAL DETAILS

2.1. Materials

A plain woven polyester fabric (100 %, 160 g/m²) was used as the main substrate in the experimental trials. The warp and weft densities of the plain woven fabric were 40 ends/cm and 20 picks/cm, respectively. The fabric was supplied by DKC Technical Coating Company (Bursa,

Table 2. Properties of chemicals

Chemicals	Property
Binder (B) (Kemiteks)	Self-crosslinking pure acrylate-based polymer binder
Aerogel 1 (A1) (Cabot)	~ 8 µm particle size, hydrophobic, translucent/opaque silica based
Aerogel 2 (A2) (Cabot)	0–~80 µm particle size, hydrophobic, translucent/opaque silica based
Aerogel 3 (A3) (Cabot)	0–0.5 mm particle size, hydrophobic, translucent/opaque silica based
Thickener (Rudolf Duraner)	Neutralized polyacrylate, anionic
Anti-foaming Agent (Rudolf Duraner)	Hydrocarbons, ethoxylated fatty acids and silicic acid combination, non-ionic
Ammonia (Tekkim)	25 % purity in liquid form
Glycerine (Tekkim)	99.5 % purity in liquid form

Turkey). Aerogel powder supplied by Cabot Aerogels (Germany) was used as the main material. The acrylic binders were provided by Kemiteks (İstanbul, Turkey). Anti-foaming agent and thickener were supplied by Rudolf Duraner (Bursa, Turkey). The properties of the chemicals used in the study are shown in Table 2. All chemicals were used in as-received form without further purification.

2.2. Preparation of coating paste

For experimental studies, aerogel coating pastes were prepared by using 3 different types of aerogel powders (A1, A2, A3) with different particle sizes in 3 different concentrations (1 %, 2 %, 4 %). In addition, blind coating paste containing chemicals other than aerogel was also prepared as a reference. Thus, a total of 10 different paste formulations were obtained. The pH values of the coating pastes were adjusted to 9.5–10 using ammonia. The viscosity of the coating pastes was measured by SOIF NDJ 6 Digital Viscometer and was varied in the range of 8000 ± 500 cP. Coating paste formulations are indicated in Table 3.

Table 3. Blind (reference) and aerogel coating paste formulations

Chemicals	B*	1 %	2 %	4 %
	g/kg	g/kg	g/kg	g/kg
Binder (B)	300	300	300	300
Aerogel powder (A1, A2, A3)	0	10	20	40
Antifoam	20	20	20	20
Glycerine	20	20	20	20
Water	620	610	600	580
Thickener	20	20	20	20
Ammonia (25%)	20	20	20	20
Total	1000	1000	1000	1000

*B: Blind (reference)

2.3. Coating, drying and curing processes

Polyester fabrics were coated knife-on-roll method with blind and aerogel coating pastes. Coating processes were realized at laboratory type ATAC GK 40 RKL (İstanbul, Turkey) compact coating machine. The distance between the knife and roll was arranged as 0.3 mm and the value was checked to be constant before each coating process. The coated samples were dried at 100 °C for 5 min and then cured at 150 °C for 4 min on the same machine. The coating procedure of the fabrics is shown in Fig. 2. Each coated fabric sample was encoded as indicated below (Table 4).

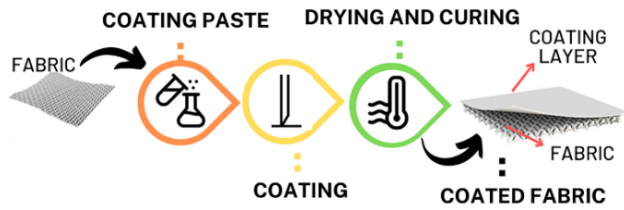


Fig. 2. Coating procedure of aerogel powders

Table 4. Sample codes of coated fabrics

Sample code	Content
U	Uncoated fabric
B	The chemicals except aerogel
A1-1	1 % A1 aerogel powder content
A1-2	2 % A1 aerogel powder content
A1-4	4 % A1 aerogel powder content
A2-1	1 % A2 aerogel powder content
A2-2	2 % A2 aerogel powder content
A2-4	4 % A2 aerogel powder content
A3-1	1 % A3 aerogel powder content
A3-2	2 % A3 aerogel powder content
A3-4	4 % A3 aerogel powder content

2.4. Scanning electron microscopy (SEM) image analysis

Scanning electron microscopic (SEM) images of the blind-coated and aerogel-coated fabrics with the same concentration (4 %) of the A1, A2 and A3 were obtained by Carl Zeiss/Gemini 300 (Jena, Germany). The blind-coated and aerogel-coated fabrics' surface images magnification rates were set to 100x, and cross-sectional images magnification rates were set to 150x.

2.5. Mass per unit area, dry add-on and thickness

Thickness and mass per unit area measurements were carried out according to TS 7128 EN ISO 5084 and TS 251 standards. Thickness (h) measurements were performed by James Heal R&B Cloth Thickness Tester (Halifax, England). Coating paste dry add-on rates ($W(\%)$) was calculated according to Eq. 1

$$W(\%) = \left(\frac{w_c - w_{uc}}{w_{uc}} \right) * 100, \quad (1)$$

where w_{uc} is the weight of the uncoated fabric; w_c is the weight of the coated fabric.

2.6. Yellowness index

The yellowness index values of the fabrics were measured by Konica Minolta CM-3600D (Tokyo, Japan)

model spectrophotometer, based on the ASTM E313 standard. The blind-coated fabric was taken as a reference in the evaluation of the yellowness index of the aerogel-coated fabrics.

2.7. Solar measurements

The solar behavior of all coated samples was measured with a Shimadzu UV-3600 Plus (Kyoto, Japan) UV/Vis/NIR spectrophotometer at a wavelength of 280-2500 nm according to EN 14500:2008. Barium Sulphate was used as a white reference surface following the standard. Solar transmittance (T_s), solar reflection (R_s), solar absorbance (A_s), and near-infrared reflectance (R_{NIR}) values were calculated according to EN 410 standards.

2.8. Thermal conductivity tests

Thermal conductivity and thermal resistance measurements of the blind-coated and aerogel-coated samples were carried out by Alambeta Testing Device which was supplied by Sensora (Liberec, Czech Republic). Thermal conductivity (λ) is the amount of heat transferred from a unit thickness of fabric to a unit surface area under the specified temperature gradient [28]. The thermal conductivity coefficient is calculated by the following Eq. 2.

$$\lambda \text{ (W/mK)} = \frac{Q}{A \frac{\Delta T}{h}}, \quad (2)$$

where, λ is the thermal conductivity coefficient(W/mK); ΔT is the temperature difference; Q is the heat transfer; A is the surface area; h is the fabric thickness.

Thermal resistance (R) expresses the temperature difference corresponding to the unit area of the material in the unit heat energy flow passing through a unit thickness fabric per unit time. This parameter is directly proportional to the material thickness and is calculated by Eq. 3 [28]. The high thermal resistance provides low heat loss.

$$R \text{ (m}^2\text{K/W)} = \frac{h}{\lambda}, \quad (3)$$

where R is the thermal resistance(m²K/W); h is the material thickness; λ is the thermal conductivity coefficient [28].

3. RESULTS AND DISCUSSION

3.1. Optical microscopy images

Optical images of the fabric surfaces are given in Fig. 3. Polyester threads are clearly visible in the images of uncoated (U) and blind-coated (B) fabrics.

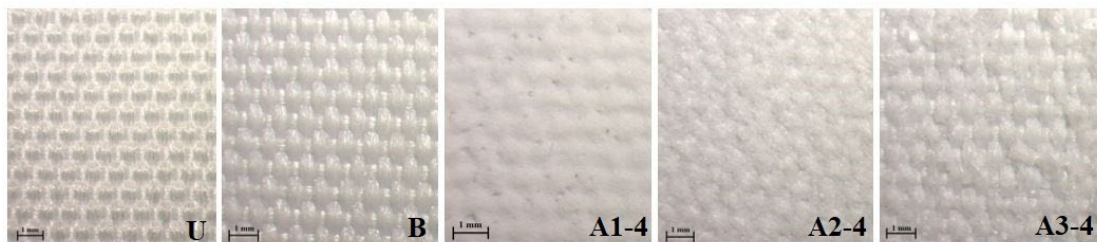


Fig. 3. Optical microscopy images: U – uncoated fabric; B – blind coated fabric; A1-4 – coated with A1 at 4 %; A2-4 – coated with A2 at 4 %; A3-4 – coated with A3 at 4 %

However, in the samples covered with aerogel powders, the yarns cannot be seen clearly because the fabric surface is covered with aerogel particles.

3.2. Scanning electron microscopy (SEM) image analysis

The surface morphology images and the cross-sectional images of the blind-coated and aerogel-coated fabric samples were examined by SEM. The images were given in Fig. 4 and Fig. 5.

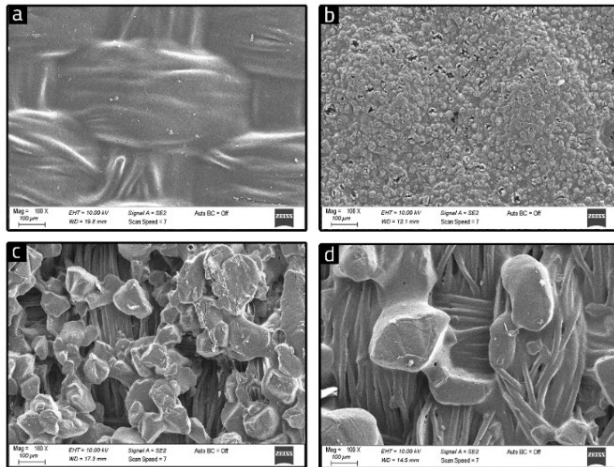


Fig. 4. SEM surface images of blind and 4 % aerogel-coated fabrics: a – blind coated; b – coated with A1; c – coated with A2; d – coated with A3

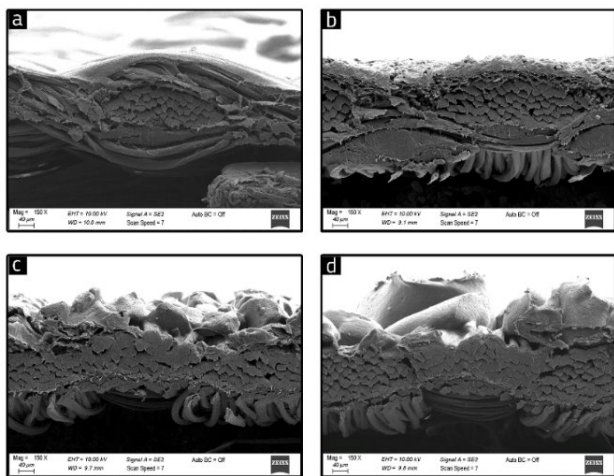


Fig. 5. SEM cross-sectional images of blind and 4% aerogel-coated fabrics: a – blind coated; b – coated with A1; c – coated with A2; d – coated with A3

The coating layers on blind-coated and aerogel-coated fabrics are clearly visible in these figures. Fig. 4 shows that the fabric surface coated with the smallest particle size A1 aerogel (Fig. 4 b) is smoother and the aerogel particles show a more homogeneous distribution. However, as the particle size increases (i.e. A2 and A3 aerogels), the number of aerogel particles per unit area on the fabric surface decreases and the empty spaces without aerogels increase. On the other hand, the cross-sectional images in Fig. 5 showed that with increasing particle size, the thickness of coating layers, unevenness, and surface roughness gradually increased.

3.3. Mass per unit area, dry add-on and thickness results

The mass per unit area and dry add-on results of fabrics coated with blind paste and different concentrations of aerogels of different particle sizes are given in Fig. 6. The results show that the blind-coated fabric with a mass per unit area of 200 g/m² is slightly higher than the results for aerogel-coated fabrics, which are generally in the range of 190–197 g/m². These differences are due to the higher density value of binder polymer compared to aerogels. Because, while the blind coating film contains only binder polymer, while the films on aerogel-coated fabrics contain binder and aerogel powders. On the other hand, no significant change is observed in the mass per unit area and dry add-on values of the aerogel-coated samples with the change in both particle size and concentration.

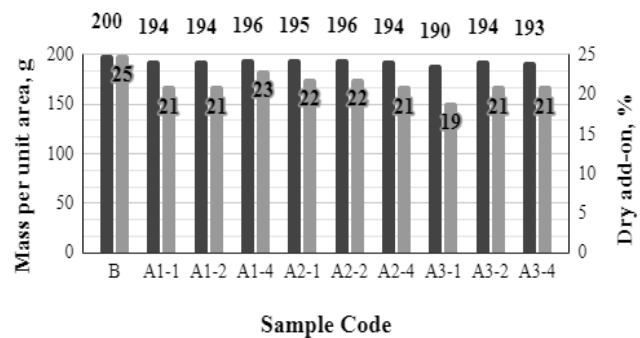


Fig. 6. Mass per unit area and dry add-on results of blind-coated and aerogel-coated fabrics

The thickness values of the coated fabrics (Fig. 7) reveal that the coating thickness regularly increases as the particle size and concentration of the aerogels increase. Accordingly, the highest thickness value was obtained with 4 % concentration of the A3 aerogel, which has the largest particle size. This result is in good agreement with the results in Fig. 5, where a variation in coating thickness is related to the aerogel particle size.

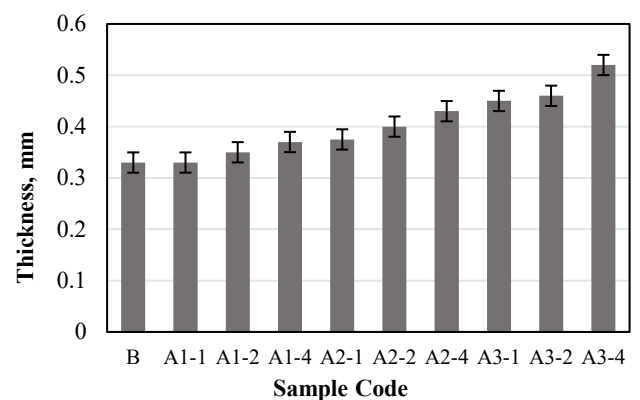


Fig. 7. Thickness results of blind-coated and aerogel-coated fabrics

3.4. Yellowness index results

A yellowing effect was observed after the high-temperature fixation of the coated fabrics. This effect was evaluated by measuring the yellowness index values of blind and aerogel-coated fabrics according to ASTM E313-73 standard. The yellowness index values seen

in Fig. 8 reveal that the yellowing effect of blind-coated fabrics is significantly higher than that of aerogel-coated fabrics. This difference can be explained by the fact that yellowing actually occurs in the coating polymers since the aerogel powders are stable to high temperatures [29]. On the other hand, a previous study has revealed that the binder polymer used in the coating turns yellow significantly depending on the heat treatment temperature, and it supports that the yellowing occurring here is due to the binder polymer [30]. At the lowest concentration (i.e. 1 %), approximately similar yellowness index values are obtained for all three particle sizes, and in general, as the aerogel concentration increases, the yellowness index values decrease at different rates. Depending on the increase in the concentration, the yellowness values of the fabrics coated with A1 aerogel decrease significantly, while the decrease in the yellowness values of the fabrics coated with A2 and A3 aerogels is quite limited. This difference is because the fabric surfaces covered with A1 aerogel, which has the smallest particle size, are more homogeneously and properly covered with aerogel powders. Therefore, it can be concluded that as the aerogel concentration increases, the yellowing of the coating polymer is more effectively masked by the whiter aerogel powders.

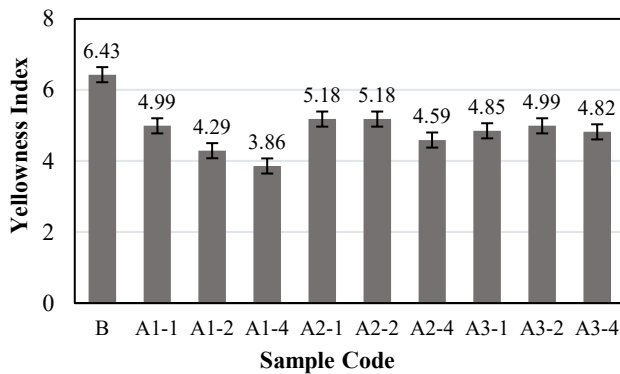


Fig. 8. Yellowness index results of blind-coated and aerogel-coated fabrics

3.5. Solar measurements results

The effect of aerogel particle size and concentration on the solar properties of coated fabrics was measured according to the EN 410 standard test method and is listed in Table 5. The table shows the effect of aerogel coatings on solar transmittance (T_S), solar reflectance (R_S) and solar absorption (A_S), as well as UV transmission (T_{UV}) and near-infrared (R_{NIR}) reflectance properties (800–2500 nm). When the results in Table 5 and Fig. 9 are examined, the A_S ,

Table 5. Results of solar properties of blind-coated and aerogel-coated fabrics

Aerogel code	Aerogel concentration, %	R_{NIR} , %	R_S , %	A_S , %	T_S , %	T_{UV} , %
B	0	60.28	61.14	5.39	33.46	7.12
A1	1	64.97	66.12	4.78	29.10	5.79
	2	70.78	72.24	2.86	24.90	4.57
	4	76.33	77.91	1.37	20.72	3.63
A2	1	61.9	62.88	5.49	31.63	6.74
	2	63.05	64.00	5.12	30.88	6.33
	4	64.65	65.60	4.47	29.93	5.90
A3	1	60.66	61.52	5.68	32.80	7.03
	2	60.39	61.28	5.68	33.04	6.96
	4	60.93	61.86	5.60	32.54	6.85

T_S and T_{UV} values of the aerogel-coated fabrics increased with the increase in particle size at constant concentration, while the R_S and R_{NIR} values decreased compared to the blind-coated fabric. That is, the changes in both the increase and decrease direction are very pronounced in the A1 coated fabrics, while it decreases in A2 and there is almost no change in A3. These results are supported by the literature as there is an inverse variation between increasing particle size and reflectance [31]. It is stated that as the particle size decreases, the reflection increases [32]. In addition, the fabric coated with the smallest particle size A1 aerogel has the most homogeneous and smooth surface, as seen in the SEM images of the coated fabrics (Fig. 4 and Fig. 5), and as the concentration increases, the surface is better covered so that there are no gaps between the aerogel powders. The result is a whiter, smoother and more reflective fabric surface. Thus, the reflection of solar radiation from the coated surface increases; transmission (including UV rays) and absorption are reduced. The Kubelka-Munk theory also explains these results that when there is a certain surface roughness in powders and inhomogeneous systems, the reflectivity of the sample depends on the ratio of the absorption coefficient to the scattering coefficient ($K/S = (1-R)^2/2R$, where K and S represent the absorption and scattering coefficients, respectively, and R represents the reflection). According to the theory as the particle size increases, the penetration depth of the light will increase, so the absorption will increase and the reflectance value will decrease accordingly [33].

It is known that the NIR region of solar radiation is responsible for the heating of sun-exposed surfaces [33]. Fig. 9 shows that fabric surfaces suitably coated with aerogel can effectively reflect NIR rays, similar to total solar radiation. Here again, the fabric coated with the highest concentration (4 %) of small particle size aerogel (A1) has the highest R_S and R_{NIR} ratios and therefore a better sunscreen effect is expected. Yang et al. (2013) stated in their study that the scattering coefficient largely depends on the microstructure of the coatings, namely the pore size, porosity and pore distribution, which significantly affect the thermal radiation heat transfer within the coating [34].

3.6. Thermal conductivity and thermal resistance results

The thermal insulation properties of the aerogel-coated fabrics were evaluated with the thermal conductivity (λ) given in Fig. 10 and the thermal resistance (R) results given in Fig. 11.

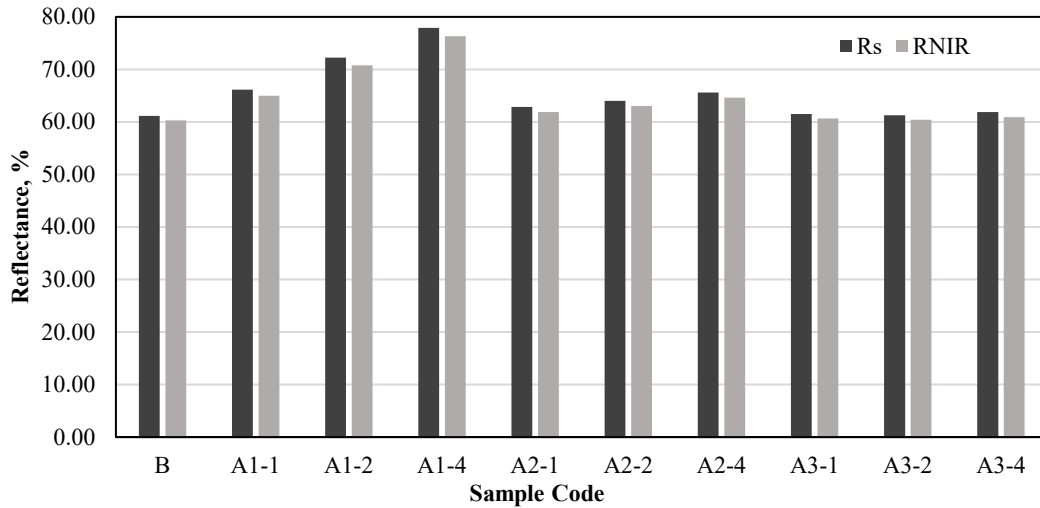


Fig. 9. Reflectance values of blind and aerogel-coated fabrics

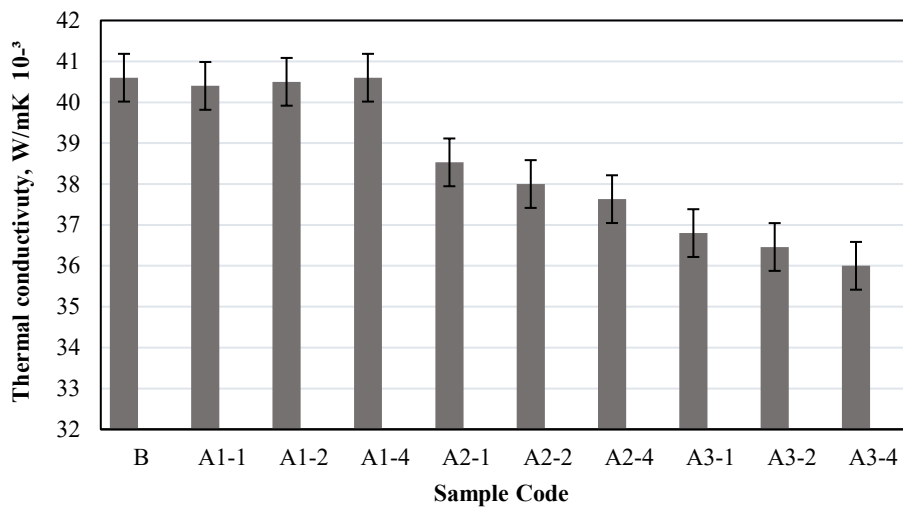


Fig. 10. Thermal conductivity results of blind-coated and aerogel-coated fabrics

As stated in the literature, if λ decreases and R increases, the thermal insulation properties of the coated surfaces improve [28]. The thermal conductivity of the blind-coated fabric (B) is reduced by aerogels as increasing the porosity which limits conductive and convective gas transport [35,36]. Fig. 10 shows that the coefficient of thermal conductivity values at a constant concentration (4 %) in different aerogel particle sizes decreases as the particle size increases. Fabrics coated with A3-4 (largest particle size) have the lowest thermal conductivity. It is known that silica aerogels provide thermal insulation due to their high porosity, and the particle size of aerogels shows the average distance between particles and has an important role in thermal conductivity [10, 11, 12]. Although there are no studies on the particle size of aerogels in textile fabrics, Chen et al. conducted a study on geopolymer foam aerogel renders for buildings. Although the results indicated that the coefficient of thermal conductivity increased with increasing particle size of the aerogels, the authors noted that larger particle size could make the aerogel better

function as a thermal insulator in the geopolymer foam renders [37].

On the other hand, it was observed that the thermal conductivity values decreased slightly in A1 and A2 and significantly decreased in A3 at constant particle size. This result is also closely related to the increase in fabric thickness and porosity. Because it is clearly seen in Fig. 6 and Fig. 7 that the thickness and porosity of the coated fabric increase regularly depending on the increase in particle size and concentration. In addition, as the aerogel particle size and concentration increase, the R values (Fig. 11) which is a coefficient depending on the fabric thickness increase (Eq. 3) [28]. Bhuiyan et al. studied on the coating of cotton fabric with aerogel at different concentrations in the presence of polyurethane binder and stated that as the aerogel concentration increased, the thermal resistance increased [22]. Therefore, since a low thermal conductivity coefficient and high thermal resistance are required for effective thermal insulation, it turns out that the best thermal insulation sample is A3-4.

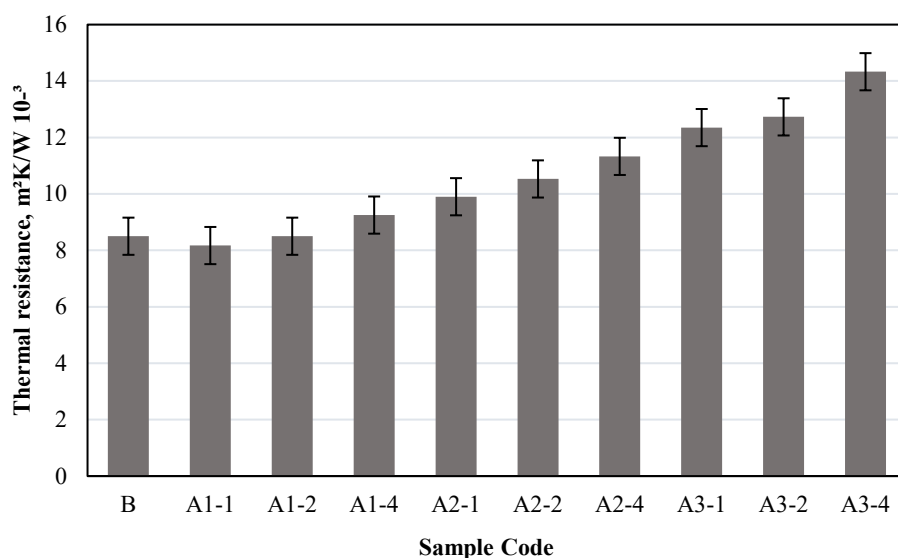


Fig. 11. Thermal resistance results of blind-coated and aerogel-coated fabrics

4. CONCLUSIONS

The main purpose of this study is to investigate the thermal and solar properties of textiles coated with silica aerogels of different particle sizes and concentrations. The 100% polyester woven fabric is coated with aerogel powders with different particle sizes and concentrations. The results were evaluated in terms of yellowness, thermal insulation, and solar properties:

1. The yellowing effect on the coated samples was not caused by the yellowing of the aerogel powders, but by the acrylic-based coating polymer used. Therefore, based on this result, it is possible to say that white aerogel powders are resistant to yellowing at fixed temperatures of around 150 °C, which are generally used in textile coatings.
2. The thermal conductivity coefficient of the aerogel-coated samples decreased as the particle size and concentration increased due to the increased porosity thickness. The lowest thermal conductivity coefficient was obtained at the highest concentration (4 %) and particle size (A3: 0–0.5 mm). At the same time, the thermal resistance values are also compatible with the thermal conductivity coefficient. The thermal resistance values are increased as particle size and concentration increase.
3. The solar property results showed that particle size and concentration effects the reflectance, absorption and transmission values. The solar absorption (A_S), solar transmission (T_S) and UV transmission (T_{UV}) values of the aerogel-coated fabrics increased with the increase in particle size at constant concentration, while the solar reflectance (R_S) and NIR reflectance (R_{NIR}) values decreased compared to the blind coated fabric. Here again, these results showed that the roughness of the surface is related to the solar properties. The highest reflectance has occurred at the smallest particle size (A1: ~ 8 μ m) at the highest concentration with a well-covered smooth surface.

Based on all the results obtained, aerogel coatings have the potential to be used in improving the thermal insulation and sun protection properties of fabrics such as curtains, awnings and tents. These results were obtained with single-layer coating and it is thought that the density of the aerogel coated on the fabric is not high enough. Since aerogel is a very light material, smooth coatings above the maximum concentration of 4 % could not be obtained in the study. Another way to increase the density of the aerogel coated on the fabric surface is to make multi-layered coatings, which studies are continuing.

Acknowledgments

The research leading to these results has received funding from the project titled "Development of Innovative Industrial Fabrics with High Thermal Insulation" in the frame of the program "Bursa Uludag University Scientific Research Projects Unit Graduate Thesis Project" under the grant agreement number FDK-2021-328. The authors thank to Bursa Uludag University for their financial support. Acknowledgment is also given to Cabot Corporation for providing aerogels, Kemiteks for providing binders, and Rudolf Duraner for providing antifoaming and thickener used in the study.

REFERENCES

1. Boukhriss, A., Cherkaoui, O., Gmouh, S. Adsorption–Desorption Kinetics of Silica Coated on Textile Fabrics by the Sol–Gel Process *Journal of Coatings Technology and Research* 17 (2) 2020: pp. 371–380. <https://doi.org/10.1007/s11998-019-00281-8>
2. Sun, D., Stylios, G.K. Fabric Surface Properties Affected by Low Temperature Plasma Treatment *Journal of Materials Processing Technology* 173 2006: pp. 172–177. <https://doi.org/10.1016/j.jmatprotec.2005.11.022>
3. Manasoglu, G., Celen, R., Kanik, M., Ulcay, Y. Electrical Resistivity and Thermal Conductivity Properties of Graphene-Coated Woven Fabrics *Journal of Applied Polymer Science* 136 (40) 2019: pp. 48024.

- <https://doi.org/10.1002/app.48024>
4. **Aral, N., Yigit, I.** Antibacterial Nonwoven with Propolis for Use in Surgical Masks *Materials Science Forum* 1063 2022: pp. 63–69.
<https://doi.org/10.4028/p-rfd11q>
 5. **Kistler, S.S.** Coherent Expanded Aerogels and Jellies *Nature* 127 (3211) 1931: pp. 741.
 6. **McNeil, S.J., Gupta, H.** Emerging Applications of Aerogels in Textiles *Polymer Testing* 106 2022: pp 107426.
<https://doi.org/10.1016/j.polymeresting.2021.107426>
 7. **Caps, R., Fricke, J.** Aerogels for Thermal Insulation. In: Aegerter, M.A., Mennig, M. (eds) *Sol-Gel Technologies for Glass Producers and Users*, Springer, Boston, MA, 2004: pp. 349–353.
https://doi.org/10.1007/978-0-387-88953-5_46
 8. **Dorcheh, A.S., Abbasi, M.H.** Silica Aerogel; Synthesis, Properties and Characterization *Journal of Materials Processing Technology* 199 2008: pp. 10–26.
<https://doi.org/10.1016/j.jmatprotec.2007.10.060>
 9. **Yilmaz, Y.** Synthesis and Characterization of Monolithic Silica Aerogel and Silica Aerogel with Sol-Gel Method by Using Different Starting Materials. Master Thesis, Gazi University, 2013: pp. 6–19.
 10. **Maleki, H., Durães, L., Portugal, A.** An Overview on Silica Aerogels Synthesis and Different Mechanical Reinforcing Strategies *Journal of Non-Crystalline Solids* 385 2014: pp. 55–74.
<https://doi.org/10.1016/j.jnoncrysol.2013.10.017>
 11. **Dai, Y.J., Tang, Y.Q., Fang, W.Z., Zhang, H., Tao, W.Q.** A Theoretical Model for the Effective Thermal Conductivity of Silica Aerogel Composites *Applied Thermal Engineering* 128 2018: pp. 1634–1645.
[10.1016/j.applthermaleng.2017.09.010](https://doi.org/10.1016/j.applthermaleng.2017.09.010)
 12. **Koebel, M., Rigacci, A., Achard, P.** Aerogel-Based Thermal Superinsulation: An Overview *Journal of Sol-Gel Science and Technology* 63 2012: pp. 315–339.
<https://doi.org/10.1007/s10971-012-2792-9>
 13. **Eas Fibers.** Insulation Materials Thermal Conductivity Coefficients. <http://tr.eas-fiberglass.net/news/Silica-Aerogel-Insulation-Blanket.html>, 2019.
 14. **Moheman, A., Showkat, A. B., Abu, T.** Aerogels for Waterborne Pollutants Purification *Advances in Aerogel Composites for Environmental Remediation* 2021: pp. 109–124.
<https://doi.org/10.1016/b978-0-12-820732-1.00007-2>
 15. **Alwin, S., Shajan, X.S.** Aerogels: Promising Nanostructured Materials for Energy Conversion and Storage Applications *Materials for Renewable and Sustainable Energy* 9.2 2020: pp. 1–27.
<https://doi.org/10.1007/s40243-020-00168-4>
 16. **Venkataraman, M., Mishra, R., Kotresh, T.M., Militky, J., Jamshaid, H.** Aerogels for Thermal Insulation in High-Performance Textiles *Textile Progress* 48 (2) 2016: pp. 55–118.
<https://doi.org/10.1080/00405167.2016.1179477>
 17. **Gao, S., Li, H., Lai, X., Zeng, X.** UV-curable Superhydrophobic Organosilicon/Silica Hybrid Coating on Cotton Fabric for Oil–water Separation *Journal of Coatings Technology and Research* 17 (5) 2020: pp.1413–1423.
<https://doi.org/10.1007/s11998-020-00362-z>
 18. **Jin, L., Hong, K., Yoon, K.** Effect of Aerogel on Thermal Protective Performance of Firefighter Clothing *Journal of Fiber Bioengineering and Informatics* 6 (3) 2013: pp. 315–324.
<https://doi.org/10.3993/jfbi09201309>
 19. **Shaid, A., Fergusson, M., Wang, L.** Thermophysiological Comfort Analysis of Aerogel Nanoparticle Incorporated Fabric for Fire Fighter's Protective Clothing *Chemical and Materials Engineering* 2 (2) 2014: pp. 37–43.
<https://doi.org/10.13189/cme.2014.020203>
 20. **Huang, D.M., Chenning, G.** Thermal Protective Performance of Silica Aerogel Felt Bedded Firefighters' Protective Clothing Under Fire Conditions *Material Science (Medziagotyra)* 23 (4) 2017: pp. 335–341.
<https://doi.org/10.5755/j01.ms.23.4.16680>
 21. **Razzaghi, M., Raeisi, H.R., Bahramian, A.R.** Improvement of Polyester Blanket Thermal Insulator Properties Using Phenolic Aerogel *Procedia Materials Science* 11 2015: pp. 522–526.
<https://doi.org/10.1016/j.mspro.2015.11.017>
 22. **Bhuiyan, M., Wang, L., Shaid, A., Shanks, A.R., Ding, J.** Polyurethane-Aerogel Incorporated Coating on Cotton Fabric for Chemical Protection *Progress in Organic Coatings* 131 2019: pp. 100–110.
<https://doi.org/10.1016/j.porgcoat.2019.01.041>
 23. **Tang, H.H., Orndoff, E.S., Trevino, L.A.** Thermal Performance of Space Suit Elements with Aerogel Insulation for Moon and Mars Exploration. No. 2006-01-2235, 2006, *SAE Technical Paper*.
 24. **North Face,** Verto S8K Model Boots. <https://www.thenorthface.com/shop/mens-vertos8k>, 2019.
 25. **Altay, P., Atakan, R., Atav, R.** Silica Aerogel Application to Polyester Fabric for Outdoor Clothing *Fibers and Polymers* 22 (4) 2021: pp. 1025–1032.
<https://doi.org/10.1007/s12221-021-0420-4>
 26. **Jabbari, M., Dan, A., Skrifvars, M., Taherzadeh, J.M.** Novel Lightweight and Highly Thermally Insulative Silica Aerogel-Doped Poly(Vinyl Chloride)-Coated Fabric Composite *Journal of Reinforced Plastics and Composites* 34 (19) 2015: pp. 1581–1592.
<https://doi.org/10.1177/0731684415578306>
 27. **Miśkiewicz, P., Tokarska, M., Frydrych, I.** Application of Coating Mixture Based on Silica Aerogel to Improve Thermal Protective Performance of Fabrics. *AUTEX Research Journal*, 2022.
<https://doi.org/10.2478/aut-2022-0003>
 28. **Mishra, R., Militky, J., Venkataraman, M.** Nanoporous Materials. In: Mishra, R., Militky, J., (ed.) *Nanotechnology in Textiles*, Woodhead Publishing, 2018: pp. 311–353.
<https://doi.org/10.1016/B978-0-08-102609-0.00007-9>
 29. **Uddin, A.J.** Coatings for Technical Textile Yarns. In: Alagirusamy, R., Das, A., (ed.) *Technical Textile Yarns*, Woodhead Publishing, 2010: pp. 140–184.
<https://doi.org/10.1533/9781845699475.1.140>
 30. **Manasoglu, G., Kanik, M., Yildirim, K.** Effect of Fixation Conditions on Yellowing Behavior of Cellulose Powder–Coated Fabrics *Journal of Engineered Fibers and Fabrics* 14 2019: pp. 1–14.
<https://doi.org/10.1177/1558925019829049>
 31. **Myers, T.L., Brauer, C.S., Su, Y.F., Blake, T.A., Tonkyn, R.G., Ertel, A.B., Johnson, T.J., ve Richardson, R.L.** Quantitative Reflectance Spectra of Solid Powders as a Function of Particle Size *Applied Optics* 54 (15) 2015: pp. 4863–4875.
<https://doi.org/10.1364/AO.54.004863>
 32. **Sun, Z., Lv, Y., Tong, Z.** Effects of Particle Size on Bidirectional Reflectance Factor Measurements from

Particulate Surfaces *Optics Express* 24 (6)
2016: pp. A612–A634.
<https://doi.org/10.1364/OE.24.00A612>

33. **Fang, V., Kennedy, J.V., Futter, J., Manning, J.** A review of Near Infrared Reflectance Properties of Metal Oxide Nanostructures *GNS Science* 2013: pp. 1912–1918.
<https://doi.org/10.1021/jp0666363o>
34. **Yang, G., Zhao, C.Y., ve Wang, B.X.** Experimental Study on Radiative Properties of Air Plasma Sprayed Thermal Barrier Coatings *International Journal of Heat and Mass Transfer* 66 2013: pp. 695–698.
<https://doi.org/10.1016/j.ijheatmasstransfer.2013.07.069>
35. **Buratti, C., Merli, F., Moretti, E.** Aerogel-based materials for building applications: Influence of granule size on thermal and acoustic performance *Energy and Buildings* 152 2017: pp. 472–482.
<https://doi.org/10.1016/j.enbuild.2017.07.071>
36. **Wei, G., Liu, Y., Zhang, X., Du, X.** Radiative Heat Transfer Study on Silica Aerogel and its Composite Insulation Materials *Journal of Non-Crystalline Solids* 362 2013: pp. 231–236.
<https://doi.org/10.1016/j.jnoncrysol.2012.11.041>
37. **Chen, Y.X., Klima, K.M., Brouwers, H.J.H., Yu, Q.** Effect of Silica Aerogel on Thermal Insulation and Acoustic Absorption of Geopolymer Foam Composites: The Role of Aerogel Particle Size *Composites Part B: Engineering* 242 2022: pp. 110048.
<https://doi.org/10.1016/j.compositesb.2022.110048>



© Koken et al. 2023 Open Access This article is distributed under the terms of the Creative Commons Attribution 4.0 International License (<http://creativecommons.org/licenses/by/4.0/>), which permits unrestricted use, distribution, and reproduction in any medium, provided you give appropriate credit to the original author(s) and the source, provide a link to the Creative Commons license, and indicate if changes were made.